Detection of VHE γ-radiation from Mkn 421 with the first two imaging Cherenkov telescopes of the HEGRA collaboration

D. Petry[a], S.M. Bradbury[a], A. Konopelko[b], J. Fernandez[a,c], F. Aharonian[b,d], A.G. Akhperjanian[b,d], F. Arqueros[c], A.S. Beglarian[d], H.G. Börst[e], J. Cortina[c], A. Daum[b], T. Deckers[e], E. Faleiro[c], E. Feigl[a], V. Fonseca[c], B. Funk[f], J. Gebauer[a], J.C. Gonzalez[c], W. Greve[e], V. Haustein[g], G. Heinzelmann[g], G. Hermann[b], M. Hess[b], A. Heusler[b], I. Holl[a], W. Hofmann[b], R. Kankanian[b], A. Karle[a,1], O. Kirstein[e], C. Köhler[b], H. Krawczynski[g], F. Krennrich[a,2], H. Kornmayer[a], A. Lindner[g], E. Lorenz[a], N. Magnussen[f], L.C. Martinez[c], S. Martinez[c], V. Matheis[b], M. Merck[a,3], H. Meyer[f], R. Mirzoyan[a,c,d], H. Möller[f], A. Moralejo[c], N. Müller[e], L. Padilla[c], M. Panter[b], R. Plaga[a], A. Plyasheshnikov[b], J. Prahl[g], C. Prosch[a], G. Rauterberg[e], W. Rhode[f], D. Renker[4], V. Sahakian[b], M. Samorski[e], J.A. Sanchez[c], K. Sauerland[e], P. Sawallisch[a], D. Schmele[g], E. Smarsch[e], R.N. Sooth[f], W. Stamm[e], M. Ulrich[b], H.J. Völk[b], S. Westerhoff[f], B. Wiebel-Sooth[f], C.A. Wiedner[b], M. Willmer[e], H. Wirth[b]

[a] *Max-Planck-Institut für Physik, München, Germany*
[b] *Max-Planck-Institut für Kernphysik, Heidelberg, Germany*
[c] *Facultad de Ciencias Fisicas, Universidad Complutense, Madrid, Spain*
[d] *Yerevan Physics Institute, Yerevan, Armenia*
[e] *Inst. für Kernphysik, Universität Kiel, Germany*
[f] *Fachbereich Physik, BUGH Wuppertal, Germany*
[g] *II. Inst. für Experimentalphysik, Universität Hamburg, Germany*

Abstract

A detection of γ-rays from Mkn 421 at energies above 1 TeV is reported. The preliminary results presented here are based on 37.2 hours of ON-Source observations with Telescope 1 (CT1) and 60.0 hours of ON-Source observations with Telescope 2 (CT2) taken between 29 December 1994 and 5 May 1995 at zenith angles up to 45°. The data were taken in ON/OFF mode such that a matching set of OFF-Observations exists. Using a standard Hillas image parameter analysis, 144 excess gamma candidates are obtained from the total CT1 data set (significance 4.0 σ) and 335 from the total CT2 data set (significance 4.3 σ).

The excess is spread over all observation periods with a rate peak in the third observation period (data from MJD of sunset 49769 until 49781) and is consistent for both CTs. For zenith angles $< 25°$, the average excess rate is 4.3 ± 1.0 h^{-1} for CT1 and 6.2 ± 1.4 h^{-1} for CT2.

A first comparison of the CT2 data at zenith angles $< 25°$ with Monte Carlo data indicates a flux of $1.4(\pm 0.32)_{\mathrm{Stat}}(+0.6-0.4)_{\mathrm{Syst}} \times 10^{-11}$ cm^{-2}s^{-1} above 1 TeV assuming a power law spectrum with index 2.0 ± 0.2.

[1] present address: DESY Institut für Hochenergiephysik, Zeuthen, Germany
[2] present address: Iowa State University, Ames, USA
[3] present address: Max-Planck-Institut für Extraterrestrische Forschung, Garching, Germany
[4] Paul-Scherrer-Institut, Villigen, Switzerland

1 Introduction

The HEGRA collaboration is operating two imaging Cherenkov telescopes in its cosmic ray detector complex [1] at the site of the Observatorio del Roque de los Muchachos on the Canary Island of La Palma (28.75° N, 17.89° W, 2200 m a.s.l.), two more telescopes are being installed at the moment and another two will follow. Data from about two years of atmospheric Cherenkov observations is already available. Among the objects observed are the Crab Nebula and the active galaxy Mkn 421.

Being the nearest BL Lac object (redshift $z = 0.0308$), Mkn 421 has been studied by many authors in all wavebands. The attention of the cosmic ray community was drawn to it when the EGRET experiment aboard CGRO reported its detection in the 50 MeV to 10 GeV range [2]. Shortly after, the Whipple group announced their detection of gamma radiation from Mkn 421 between 0.5 and 1.5 TeV at a confidence level of 6.3 σ from 7.5/7.5 hours of on/off-source observations [3]. This detection is so far unconfirmed by another experiment.

The HEGRA collaboration's Cherenkov Telescopes 1 and 2 (for a description see [4], [5] and e.g. [6]; the main technical data are summarized in table 1) have energy thresholds of about 1.5 TeV and 1 TeV respectively. Hence, they are good probes for the upper end of the Mkn 421 spectrum near the expected onset of gamma absorption effects due to the infrared background (see e.g. [7]).

Recently [8] (see also [9]), the Whipple collaboration reported having seen two burstlike increases in the flux from Mkn 421, each on a timescale of a few days, between 10 May 1994 and 12 June 1994. During this period Mkn 421 was also observed from the HEGRA site, but most of the data was taken at zenith angles greater than 30°. A preliminary analysis of this data has shown no significant excess.

Since this outburst, Mkn 421 is believed to have been emitting at a quiescent level of about half its discovery level. Results reported by the Whipple group at the ICRC 1995 in Rome [10] indicate that there were new outbursts during the first months of 1995, i.e. during the period covered by this work. The correlation between the signals observed by Whipple and our signals still has to be examined.

2 Observations and data analysis

The observations made during the first months of 1995 were analysed in four steps: (1) preselection based on the general information about weather and the status of the telescopes, (2) flat fielding and calibration of the PMT signals, (3) filtering of the remaining data to obtain a dataset of showers with well determined image parameters ALPHA, CONC, WIDTH, LENGTH etc. (for a definition of the Hillas image parameters see e.g. [11]), (4) selection of gamma candidates using cuts on the image parameters.

2.1 Selection and analysis of data from Telescope 2

In the period from 29 December 1994 to 5 May 1995 we recorded 91 hours of ON-source observations of Mkn 421 with the HEGRA collaboration's Cherenkov Telescope 2. In a 23 minutes ON/OFF or OFF/ON rhythm, matching OFF-source observations were made. Neither the ON- nor the two OFF-source positions contain bright stars. The observations were made at zenith angles between 9° and 55°.

	Telescope 1	**Telescope 2**
Nominal Energy Threshold[5]	estimated 1.5 TeV	1.1 ± 0.1 TeV
Av. Trigger Rate ($Z^\circ = 0^\circ$)	1.4 Hz	3.1 Hz
Distance	92.5 m	
Mount		
Type	equatorial	alt-azimuth
Tracking Accuracy	$\pm 0.1^\circ$	
Mirrors		
Shape	spherical	
Material	aluminized glass, 2 cm thick, SiO_2 coated	
Diameter	60 cm	
Total Number	18	30
Total Area	5 m^2	8.5 m^2
Focal Length	492 ± 4 cm	
Angular Resolution	20 - 40 arcsec	
Reflectivity	$> 84\%$ ($300\mathrm{nm} \leq \lambda \leq 600\mathrm{nm}$)	
Camera		
Photomultiplier	type EMI-9083A (10 stage)	type FEU-130 (12 stage)
Quantum Efficiency at 375 nm	26 %	19 %
Light Guide	hollow Winston Cone	plexiglass Winston Cone
Entrance Window shape	hexagonal, 21 mm diam.	hexagonal, 36 mm diam.
Angular pixel diameter	0.25°	0.43°
Number of Pixels	127	61
Field Of View	3.25°	3.9°
Light Collection Efficiency in focal plane	$\approx$ 90 %	$\approx$ 80 %
Calibration	337 nm N_2-Laser (3 ns pulse) + quartz fiber + NE-111 scintillator (6 mm thick)	
Readout		
Trigger Condition	$2/127 \geq$ thresh. within 13 ns	$(2/61 + 1/37) \geq$ thresh. within 13 ns
ADC Gate Width	30 ns	
Dead Time	2.5 ms	1.2 ms

Table 1: The main technical data of the first two telescopes of the HEGRA collaboration

From the total 2×91 hours of observations, 161 ON/OFF pairs (= 62 h ON/62 h OFF) were selected on the basis of weather information recorded by the observers and nightly extinction measurements from the Carlsberg Automatic Meridian Circle near the HEGRA site. They correspond to 679098 events ON and 678293 events OFF.

[5]This is E_{thr} as defined in section 4 for $\alpha = 2.0 \pm 0.2$ and zenith angle 15°. For CT2, after all cuts described in section 2 and a gamma source flux with differential spectral index 2.7, the maximum of the expected differential gamma rate is at 1.8 ± 0.6 TeV (error due to uncertainty in absolute energy calibration)

2.1.1 Flat fielding

Before each run, a set of 500 random triggers called a *pedestal run* is recorded. From this data, the pedestal and the noise of each pixel is determined as the mean and the standard deviation excluding signals above and below 6 standard deviations and iterating three times.

Before each series of runs, the gain of the photomultipliers is calibrated by recording the camera response to 100 shots of a pulsed light source with $< \lambda > = 370$ nm at the center of the telescope dish, 5 m away from the camera. The light source is formed by a small piece of NE-111 scintillator being excited by an N_2 laser via an optical fibre. From these 100 signals the mean is calculated for each pixel. The ratio of this mean and the mean of the signals over *all* pixels is then used to normalize the raw signals recorded in the observations.

2.1.2 Filtering

Several consistency checks and quality cuts were applied:

1. The camera of CT2 has a hexagonal field of view with 3.9° diameter consisting of 4 rings of hexagonal 0.43° diameter pixels round a central pixel. The 61 pixels have plexiglas light guides in which penetrating muons radiate Cherenkov light. These can fake gamma-like events of low WIDTH. To overcome this problem an anti-coincidence shield consisting of a scintillator barrel around the camera and attached photomultipliers is used (for a brief description see [12]). An event was rejected when one of these photomultipliers gave a signal of more than 3 standard deviations above its pedestal. This cut eliminates depending on the zenith angle up to 15 % and on average 5 % of the raw events (see figure 1).

2. The hardware trigger condition of CT2 is "(2 out of 61 > 60 mV) AND (1 out of 37 > 60 mV)" where 60 mV is the discriminator level and 37 means all pixels except the outermost ring. This corresponds on average to 34 - 6 ADC counts where the error is the downwards fluctuation due to differences in the light arrival time.

   Because of the well known asymmetry of the images of gamma showers coming from a point source at the center of the camera, events which have their triggering pixels in the outer ring of the camera are truncated by the camera edge and thus have badly determined image parameters. This situation can be improved by applying a software trigger which only uses the inner 37 pixels and not the outermost ring (pixels 38 - 61)[6].

   Furthermore, the software trigger is necessary in order to make the data more compatible to Monte Carlo simulations where a good simulation of the hardware trigger condition was not yet achieved. The condition "2 out of 37 > 34 ADC counts" was therefore applied to the calibrated signals.

   It was also suggested that software triggers fight the "muon arc" background since they imply a concentration cut for small events. This background may be a reason for concern when working very near the telecopes' hardware threshold because it could dilute the gamma ray signals and - if there are non-negligible differences in the night-sky background between ON and OFF and no software padding [13] is applied - it could

[6] In order to have a large coincidence rate with CT1, the trigger condition "2/37 > ..." is not chosen on the hardware level. The loss in coincident events which is caused by this software trigger is not problematic for this analyis since it is not trying to make use of stereoscopic methods.

result in a fake signal. This signal, however, would only show up in a *shape* parameter analysis, i.e. it would make the gain in significance from additional orientation parameter cuts (e.g. ALPHA) comparatively small.

Whether we see Muon arcs and the implications of this still have to be investigated. The improvement in significance achieved by the ALPHA cut for the total data set is in this analysis a factor of 1.8 which is near the value expected from MC simulations which do not include local muons. We therefore conclude that after the software trigger there is no significant muon arc signal component in the data sample.

3. The effect of three different zenith angle (θ) cuts on the signal were studied: $<25°$, $<35°$ and $<45°$ (which are almost equidistant in $\cos(\theta)$). The image cuts used (see below) were optimized for zenith angles $< 30°$. From an analysis with zenith angle

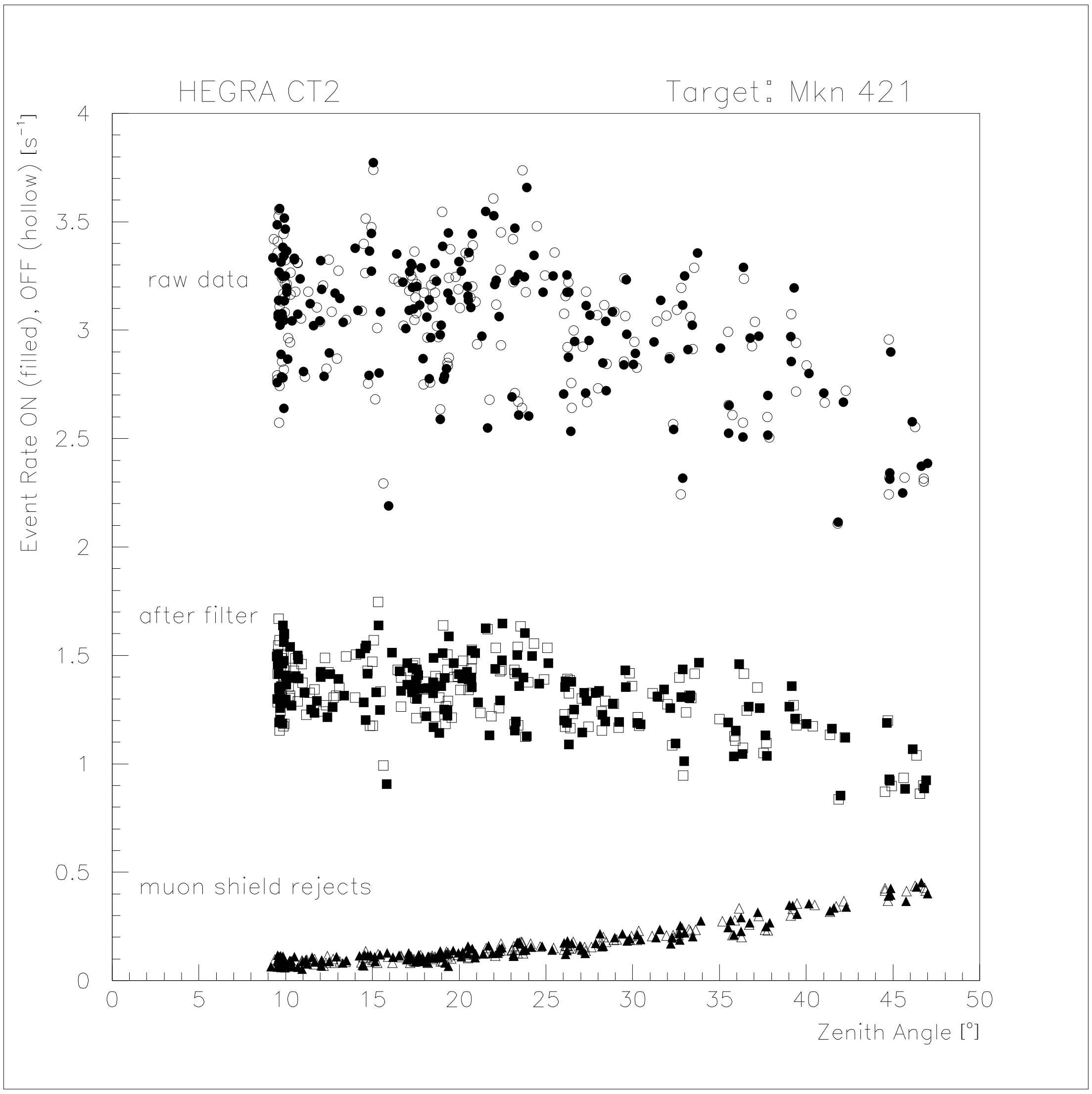

Figure 1: For each run of CT2 (filled = ON, hollow = OFF) included in this analysis, this plot shows three quantities versus the average zenith angle of the run: (a) (circles) the raw event rate, (b) (squares) event rate after filter (this is mainly the 2/37 software trigger and the muon shield), (c) (triangles) events removed by the muon shield.

dependent cuts we expect an improved significance [7].

4. Patches of data with bad pointing were detected by recalculating the source position from the shaft encoder positions for each event and comparing it to the nominal source position. Consecutive events in an ON-source-file with a deviation of more than 0.3° were removed and the difference in time between the last and the first event was subtracted from the run time. In this way 563 events were removed and 4.6 minutes of runtime were cut out. In the OFF-data, the pointing quality was monitored, too, but no events were removed. The average pointing error of the events after filter is according to this method 0.05°± 0.03° for ON and 0.08°± 0.06° for OFF.

5. In order to notice possible high trigger rates caused by artificial light sources like car headlights, a *momentary rate* was calculated using the formula

$$f(i) = \frac{2N+1}{t(i+N) - t(i-N)}$$

where $f(i)$ is the momentary rate for event i (numbering before all filters and cuts), $t(i)$ is the time at which event i occurred (accurate to 200 ns), and N is a constant which was chosen to be 60 events. The whole dataset was scanned for events with rates significantly above or below the mean rate of the corresponding run. Two runs which clearly contained artificially caused peaks were found and removed (ON and corresponding OFF).

6. After the calculation of the image parameters (see below) a concentration cut is applied to eliminate further muon induced events which may have survived the muon shield veto:

$$\mathrm{CONC} < 0.95$$

7. Very close to the position of Mkn 421 there is a 6th magnitude star which causes slightly increased anode currents in the central pixel. In order to reduce a possible trigger bias, the condition was imposed that this pixel # 1 must not have the largest signal of the image.

8. The number of pixels in the image was required to be at least 3. After all cuts except ALPHA the number of pixels in the image is on average 7.4 ± 1.9 for ON and OFF. Most of the ON source excess comes from events with between 5 and 9 image pixels.

2.1.3 Image preparation and image parameter cuts

The image preparation which precedes the image parameter cuts is a "topological two-level tailcut"[8] and consists of three steps:

1. Pixels are accepted to be part of the image if they have a calibrated signal 3.0 standard deviations above pedestal *and* which have a neighbour which satisfies the same condition. These pixels form the image core.

[7] However, with a variable source like Mkn 421 it is important to note that a change in the zenith angle cut also changes the time interval analysed since the zenith angle distribution varies from month to month. So changes in the signal and its significance seen when varying the zenith angle cut can also be caused by different degrees of activity of the source.

[8] The method described here is similar to the method described in e.g. [15] (appendix B) except here the additional condition is imposed that core pixels are required to have at least one adjacent core pixel.

2. All pixels which have a neighbour in the core *and* a calibrated signal more than 2.5 standard deviations above their pedestal are accepted into the image boundary.
3. Pixels which are neither part of the core nor the boundary are set to zero.

The values 3.0 and 2.5 were chosen from general probability considerations and not optimized. Using 60/60 hours of ON/OFF observations of the Crab Nebula (made with CT2 in 1994 at zenith angles $< 30°$) optimized cuts were obtained by [14]. When Monte Carlo data (see section 4) became available, the cut on ALPHA and the lower cuts on DIST and LENGTH were only slightly changed to correctly describe the gamma domain. The following list shows the cuts which were finally used. The original values obtained from the optimization on the Crab data are given in brackets.

$$0.6°(0.5°) < \mathrm{DIST} < 1.2°(1.2°)$$
$$0.5(0.5) < \mathrm{CONC}$$
$$0.06°(0.06°) < \mathrm{WIDTH} < 0.2°(0.2°)$$
$$0.18°(0.16°) < \mathrm{LENGTH} < 0.375°(0.375°)$$
$$\mathrm{ALPHA} < 20°(22°)$$

There is an indication from MC data that a cut at smaller ALPHA is justifyable and would improve the significance even though the resolution of the CT2 camera is relatively low (see figure 2). This is mainly dependent on the tracking accuracy. We will present here the results for the cut at 20° only.

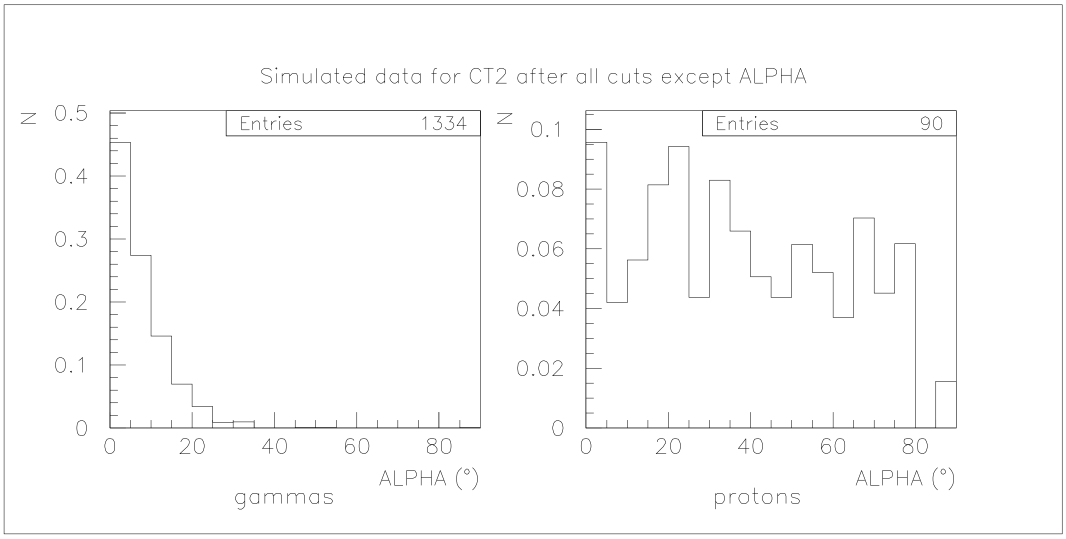

Figure 2: The distribution of the parameter ALPHA after all cuts (except ALPHA, see text) for simulated gamma induced showers (assumed differential spectral index $\alpha = 2.0$) and simulated proton induced showers (assumed $\alpha = 2.7$). For details of the simulation see section 4.

2.2 Selection and analysis of data from Telescope 1

In winter 1994/95 the first Cherenkov Telescope of the HEGRA collaboration (CT1) was equipped with a new high resolution 127 pixel camera [4]. It became operational again at the end of January 1995 and data taken between 30 January 1995 and 1 May 1995 were included in this analysis. Out of the 122 ON/OFF pairs (= 46.8 h ON/46.8 h OFF) taken in this period of time, 101 pairs (38.9 h ON/ 38.9 h OFF) were accepted, containing 189779 events ON and 191496 events OFF.

2.2.1 Flat fielding

The flat fielding and filtering of the data was done in a way very similar to that for CT2, so only the differences will be discribed.

Pedestal determination and gain calibration was done in the same way as for CT2. Due to a data aquisition software error, there were unfortunately only pedestal runs for about 50 % of the data available. For the remaining data, the pedestal and its standard deviation was determined for each pixel from the peak position and the Full Width Half Maximum of the pulse height distribution of the raw data for each run. The values obtained with this method were in very good agreement with the values obtained with the standard method for the data where pedestal runs were available.

2.2.2 Filtering

1. The new camera of CT1 [4] is equipped with open aluminium coated Winston cones which are protected by only a thin plexiglass window against dust and humidity, so events caused by direct muon hits in the camera are much less probable than for CT2. The camera is not equipped with a muon shield.
2. A software trigger 2/91 > 21 ADC counts was applied to the calibrated signals.
3. Three different zenith angle cuts were applied: θ <25°, 35° and 45°.
4. The data was checked for bad pointing (see CT2). 126 events corresponding to 2.6 minutes were cut out. The average pointing error after filter was 0.04 ± 0.02 for ON and 0.04 ± 0.03 for OFF.
5. The rate check was done as for CT2. No events had to be removed.
6. After the determination of the image parameters, events where pixel #1 had the largest signal were removed.
7. The number of pixels in the image was required to be at least 4. The ON-OFF excess after all cuts comes from events with between 4 and 15 image pixels. The average number of pixels in the excess events is 9.

2.2.3 Image preparation and image parameter cuts

As for CT2, a topological two-level tailcut was applied using 3.0 and 2.5 standard deviations for the core and the boundary cut respectively.

Since for the new camera neither data from Crab observations nor Monte Carlo data were available, the "Supercuts" developed by the Whipple group for their 91 0.25° pixel camera (see e.g. [15]) were used:

$$
\begin{gathered}
0.51^\circ < \mathrm{DIST} < 1.1^\circ \\
0.07^\circ < \mathrm{WIDTH} < 0.15^\circ \\
0.16^\circ < \mathrm{LENGTH} < 0.30^\circ \\
\mathrm{ALPHA} < 15^\circ
\end{gathered}
$$

In addition a cut $0.4 < \text{CONC}$ was applied analogous to the cuts for CT2 and taking into account the higher resolution of the camera.

As mentioned above, these cuts were developed for a different telescope and their efficiency when applied to CT1 data remains to be examined. Therefore the flux calculations presented in the results section were only done for CT2.

3 Results

3.1 Total signal

Table 2 shows the event statistics for both telescopes for zenith angle cuts at 45° and at 25°. The significances are calculated according to [16], equation 9.

Results CT1, zenith angle < 45°						
analysis stage	Time (h) ON	Time (h) OFF	events passed ON	events passed OFF	time normalized excess	significance
after filter	37.22	37.26	112701	111836	999	2.1 σ
after all cuts except ALPHA	"	"	3188	3056	136	1.7 σ
after all cuts	"	"	**725**	**582**	**144**	**4.0** σ
Results CT1, zenith angle < 25°						
analysis stage	Time (h) ON	Time (h) OFF	events passed ON	events passed OFF	time normalized excess	significance
after filter	25.62	25.65	81270	80641	723	1.8 σ
after all cuts except ALPHA	"	"	1904	1757	149	2.5 σ
after all cuts	"	"	**451**	**340**	**111**	**4.0** σ
Results CT2, zenith angle < 45°						
analysis stage	Time (h) ON	Time (h) OFF	events passed ON	events passed OFF	time normalized excess	significance
after filter	60.01	60.09	339214	340539	-872	-1.1 σ
after all cuts except ALPHA	"	"	12280	11965	332	2.1 σ
after all cuts	"	"	**3273**	**2942**	**335**	**4.3** σ
Results CT2, zenith angle < 25°						
analysis stage	Time (h) ON	Time (h) OFF	events passed ON	events passed OFF	time normalized excess	significance
after filter	40.51	40.59	240571	240694	351	0.5 σ
after all cuts except ALPHA	"	"	6945	6635	323	2.8 σ
after all cuts	"	"	**1885**	**1636**	**252**	**4.3** σ

Table 2: Event statistics for various cuts as described in section 2 for the data from both telescopes

3.1.1 Results for Telescope 1

Even though the observation time is almost 40 % smaller than that for CT2, an excess of comparable significance is obtained. The "Supercuts", although developed for the Whipple telescope, seem to work reasonably well.

After all cuts an excess of 144 events with a significance of 4.0 σ is obtained from the

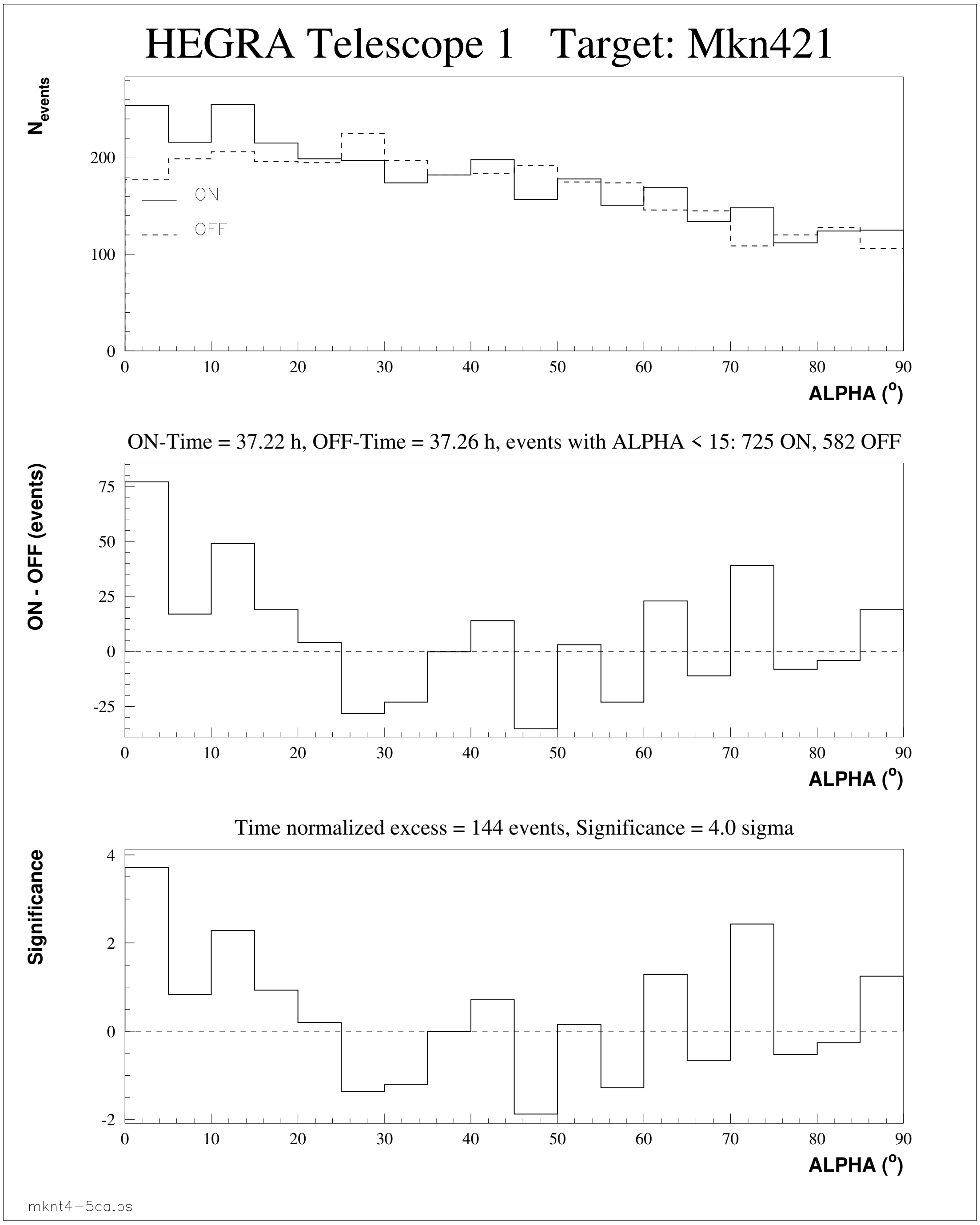

Figure 3: The distribution of the image parameter ALPHA after all cuts (except ALPHA) for the whole dataset from CT1 with zenith angle $< 45°$. Events with ALPHA $< 15°$ are regarded as gamma candidates.

total dataset above 45° zenith angle (37.22 hours of ON-observations see figure 3). This corresponds to a excess gamma candidate rate of 3.9 h^{-1}.

As is to be expected because of the lower average energy threshold, this rate rises to $4.3\,h^{-1}$ if the zenith angle cut is reduced to 25°.

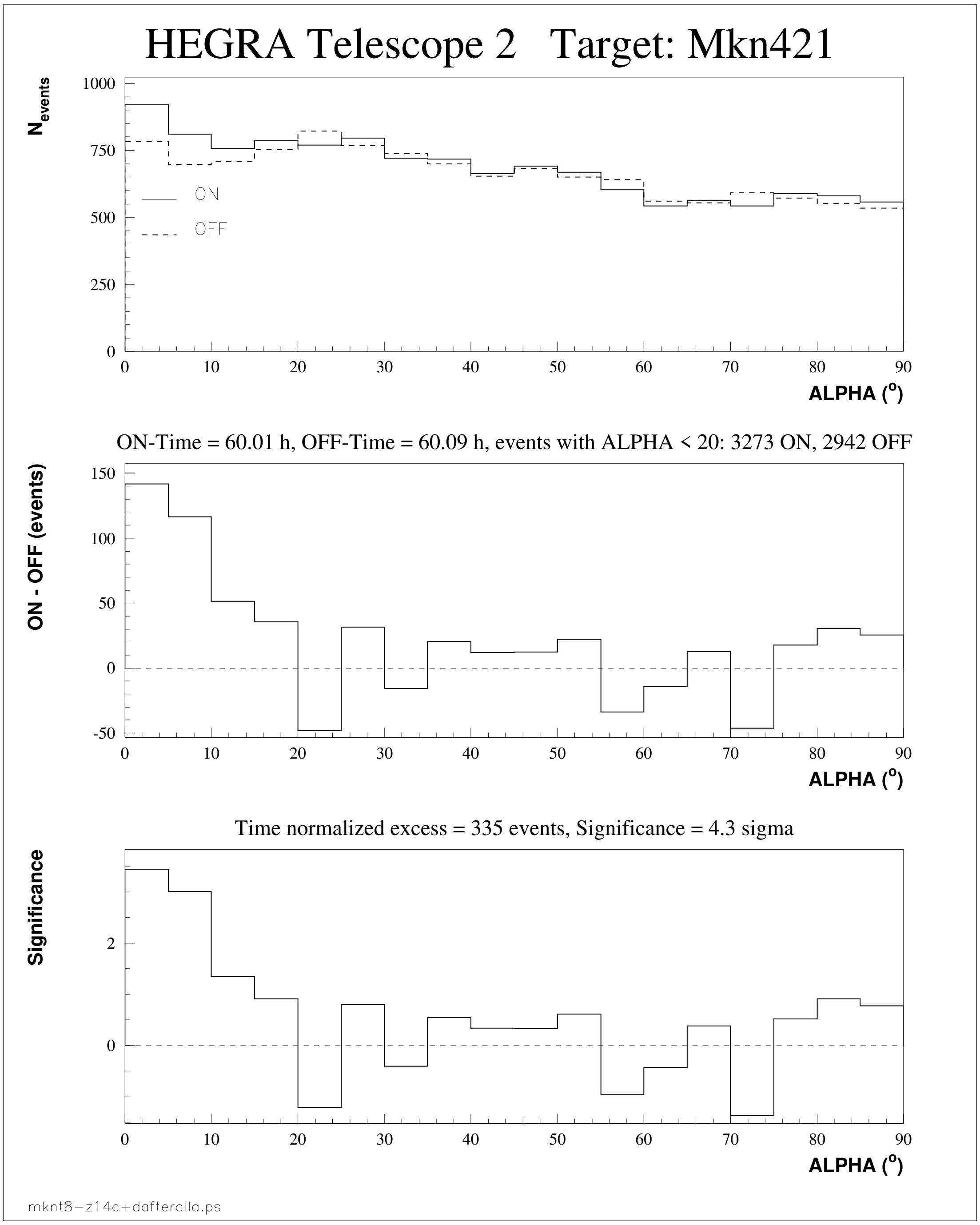

Figure 4: The distribution of the image parameter ALPHA after all cuts (except ALPHA) for the whole dataset from CT2 with zenith angle $< 45°$. Events with ALPHA $< 20°$ are regarded as gamma candidates.

3.1.2 Results for Telescope 2

For the well calibrated and better "run in" telescope 2, the signal is clearer than that for CT1: the whole dataset of 60.01 h of ON-observations above zenith angle 45° gives 335 excess events with a significance of 4.3 standard deviations (see figure 4). The excess gamma candidate rate is 5.6 h^{-1}.

A zenith angle cut at 25° leaves 40.51 h of ON-observations with 252 excess events, 4.3 σ significance. The excess rate is 6.2 h^{-1}.

3.1.3 Results for parallel observations from both telescopes

The analysis of the two datasets was strictly separated and no use has so far been made of the fact that there are 29.5 hours of *parallel* observations from CT1 and CT2 with $\theta < 45°$ in the dataset. The word "stereo observation" is deliberatly avoided here because this analysis does not try to use stereoscopic methods. The subject of this paragraph is only to examine the degree of statistical dependence of the signals seen by the two telescopes. Work on stereoscopic analysis is underway.

By restricting the data to the parallel subset (29.51 h ON/29.55 h OFF from CT1 and CT2) and applying the same analysis procedure as described above for the whole dataset, the results shown in table 3 were obtained.

Results CT1 (observations with good data from CT2), zenith angle $< 45°$							
analysis stage	events passed ON	events passed OFF	time norm. excess	signif.	Rate ON (s^{-1})	Rate OFF (s^{-1})	Rate excess (h^{-1})
after filter	91409	91026	529	1.2 σ	0.860	0.855	18
after cuts	**624**	**489**	**136**	**4.1** σ	$\mathbf{5.87 \cdot 10^{-3}}$	$\mathbf{4.60 \cdot 10^{-3}}$	**4.6**
Results CT2 (observations with good data from CT1), zenith angle $< 45°$							
analysis stage	events passed ON	events passed OFF	time norm. excess	signif.	Rate ON (s^{-1})	Rate OFF (s^{-1})	Rate excess (h^{-1})
after filter	166761	167564	-535	-0.9 σ	1.57	1.57	-19
after cuts	**1671**	**1455**	**218**	**3.9** σ	$\mathbf{1.57 \cdot 10^{-2}}$	$\mathbf{1.37 \cdot 10^{-2}}$	**7.4**
Results from events coincident within $\pm$ **1** μ**s, zenith angle** $< 45°$							
analysis stage	events passed ON	events passed OFF	time norm. excess	signif.	Rate ON (s^{-1})	Rate OFF (s^{-1})	Rate excess (h^{-1})
after filter	31611	31803	-141	-0.6 σ	**0.298**	**0.299**	-4.9
after cuts	**31**	**16**	**15**	**2.2** σ	$\mathbf{2.92 \cdot 10^{-4}}$	$\mathbf{1.50 \cdot 10^{-4}}$	**0.51**

Table 3: Results from parallel observations with good data from both telescopes

This means if both telescopes are observing in parallel, after filter about 29 % of the events from CT1 are coincident with events from CT2 after filter. The coincident rate after filter is 0.3 Hz for ON and OFF. However, after all cuts, the coincidence rates for ON and OFF differ by 50 % and are very small. 5 % of the ON events from CT1 which have survived all cuts are coincident with ON events from CT2 which have survived all cuts. For OFF this percentage is 3 % and because the absolute rates are small the ON-OFF difference has only a significance of 2.2 σ for the given dataset.

The correlation of the excess seen by CT1 and the excess seen by CT2 in this analysis is obviously small. An approximate combined significance will be calculated in the conclusion.

3.2 Time dependence of the signal

With time integrated observations of relatively small significance it is difficult to study a possible time variability. Nevertheless, in order to make our observations comparable to other observations of Mkn 421, e.g. to the data from the Whipple Observatory (about 6.5 hours behind La Palma time), the data above 35° zenith angle from each dark moon period were treated separately.

For CT2, there are 5 such observation periods in the dataset, one of which (the fourth) unfortunately contains much less good data than the other four. For CT1 there is data for only four of these observation periods since the telescope only became operational at the beginning of the second period.

Figure 5 shows the rates for both telescopes versus the Modified Julian Date of sunset. The horizontal bars indicate the formal beginning and end of each period. The error of the rate is the rate divided by the significance of the signal (the error in the time measurement is neligible). Error and rate of CT1 in this figure are scaled by a factor of 1.27 such that the average rate coincides with that of CT2.

There is a good agreement between the monthly time variability of the signals of the two telescopes which seems to be much better than one would expect from the size of the error bars.

The zenith angle cut at 35° is a compromise between using as much of the data as possible

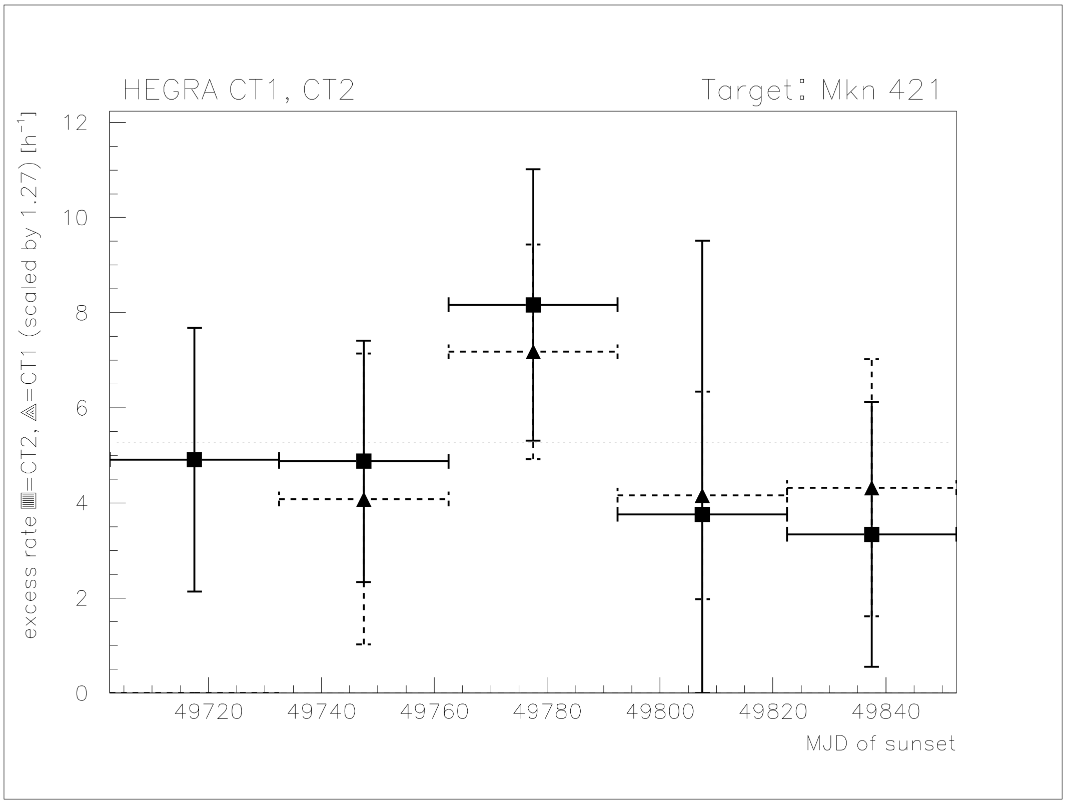

Figure 5: The excess rates for CT1 (triangles) and CT2 (squares) for the five observation periods included in this analysis for zenith angles $< 35°$. The CT1 rates were scaled to the total rate (dotted line = 5.28 h^{-1}) of CT2 by a factor of 1.27. The errorbars are the rate devided by the significance of the signal in the each observation period.

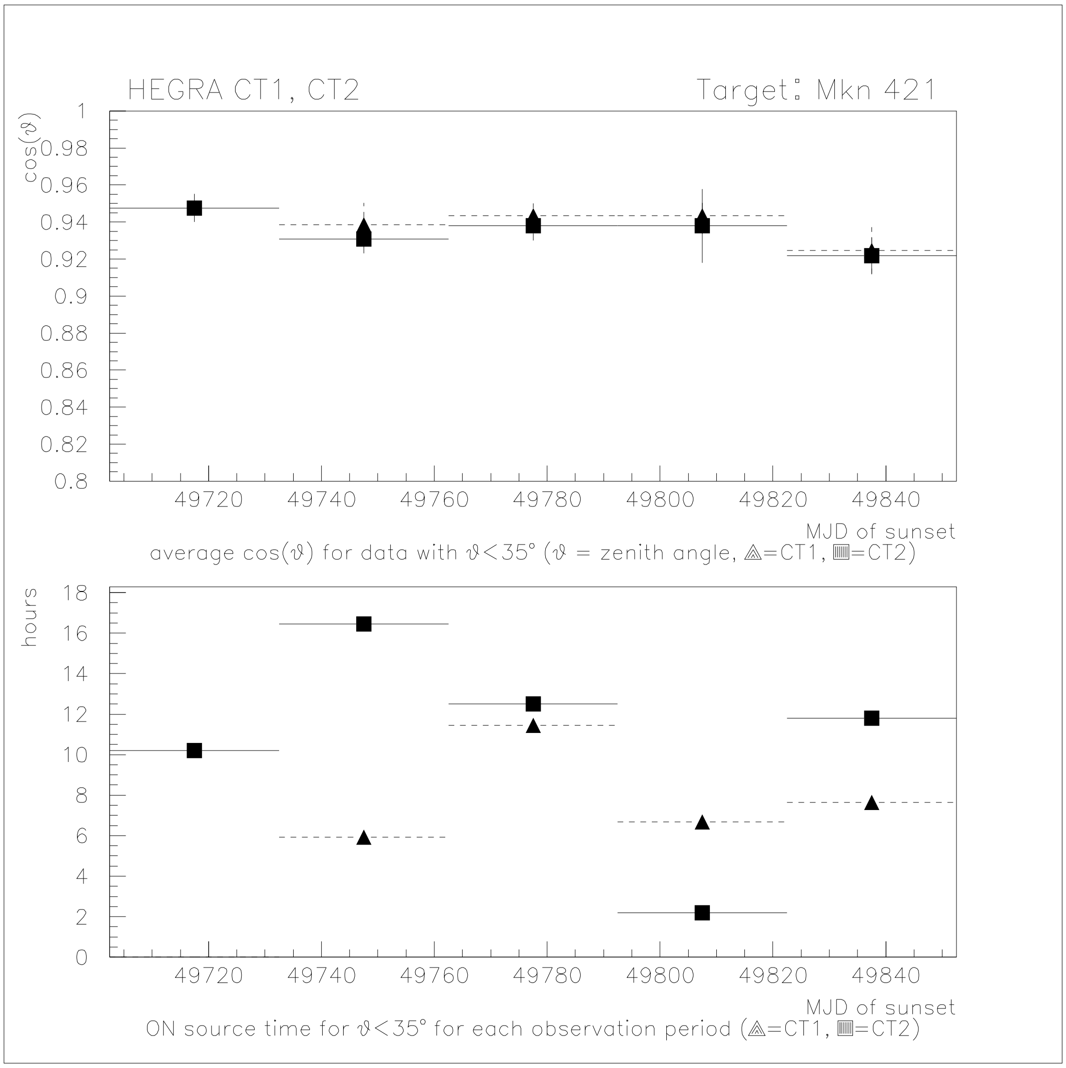

Figure 6: The average cosine of the zenith angle and the ON observation time for CT1 (triangles) and CT2 (squares) for the five observation periods included in this analysis for zenith angles $< 35°$.

and having an average energy threshold as similar as possible for all observation periods. From figure 6 it can be seen that the time averaged cosine of the zenith angle, which is a measure of the relative energy threshold, is almost the same for both telescopes and all observation periods. Variability observed can therefore only be due to technical problems so far unnoticed, changes in the atmospheric conditions, or genuine source variability. If the same variablity is seen with both telescopes, technical problems can largely be ruled out.

The rate after filter seen in OFF-source observations can be considerd as a measure of the general (especially atmospheric) conditions. Figure 7 shows this rate for the narrow zenith angle range of $15° < \theta < 20°$ averaged for each observation period. For CT2, the third observation period has both the maximum OFF-rate and the maximum excess rate, but the relative difference to the other periods is not more than a factor of 1.2 compared to a factor of 2.3 in the excess rate. This needs further investigation. The maximum of the after-filter-rate for CT1 in the second observation period, which can also be seen in figure 7, is due to a slightly higher camera high voltage in that period.

A first examination of the *daily* variability of the signal from CT2 shows that daily

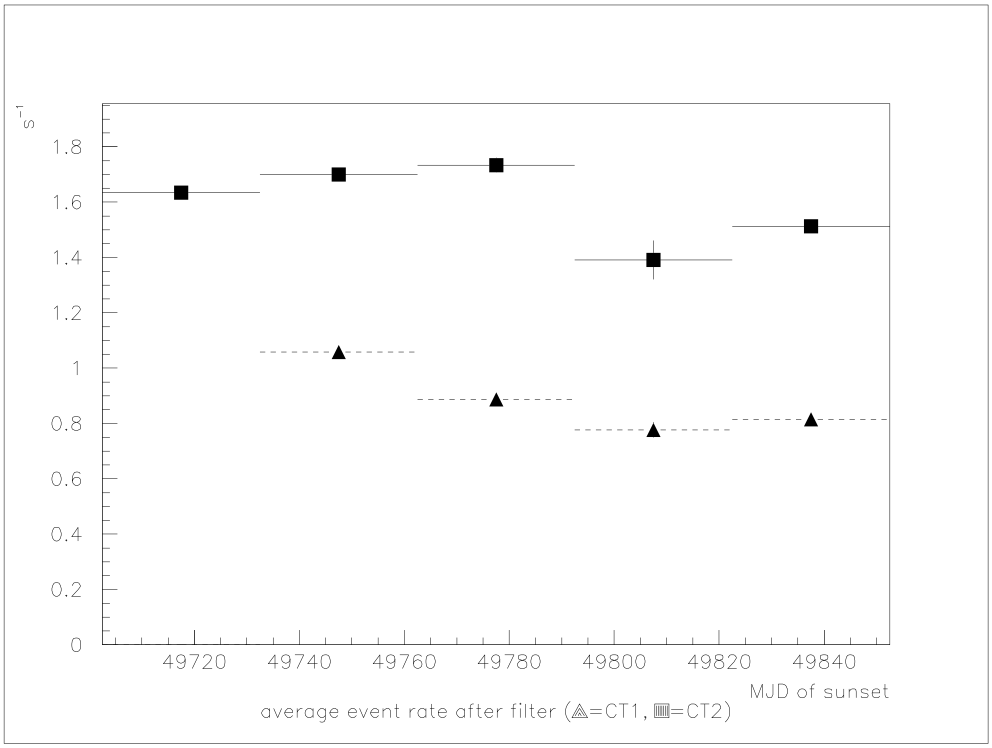

Figure 7: The average event rate after filter for *OFF-source observations* from CT1 (triangles) and CT2 (squares) for the five observation periods included in this analysis in the zenith angle range $15^\circ < \theta < 20^\circ$ as a measure for the general observing conditions.

excess rates up to 21 h^{-1} occur, but the significance of the daily excesses does not exceed 2.5 standard deviations. In fact, there are only five nights (MJD of sunset 49745, 49750, 49772, 49778 and 49833) where the significance is larger than 2 standard deviations.

4 Monte Carlo studies and flux calculations for CT2

With Monte Carlo data produced using code described in [17] (see also [19]) it was possible to arrive at a coarse determination of the average flux of Mkn 421 from the data with zenithangle $< 25^\circ$.

The databank used here consists of 27787 simulated gamma showers for 0° zenith angle, 19213 gamma showers for 30° zenith angle, 167840 proton showers for 0° zenith angle, and 45048 proton showers for 30° zenith angle with energies between 0.05 and 30 TeV.

The telescope simulation comprised the generation of Poisson random Night Sky Background similar to the real background measured in the pedestal runs and a simple simulation of the mirror imperfections performed by convoluting the camera image with a two-dimensional Gaussian with a FWHM equal to the measured point spread function of the telescope of 0.15° (value at the edge of the camera as an upper limit).

Figure 8 shows the effective collection areas after all cuts determined with this MC data. The effective collection area $A_{\text{eff}}(E_j)$ for a energy bin centered at E_j is defined here as:

$$A_{\text{eff}}(E_j) = \sum_{i=1}^{n} \varepsilon(E_j, r_i) A(r_i)$$

where n is the number of impact parameter bins used, r_i is the impact parameter corresponding to the (center of the) ith bin, $A(r_i)$ is the area of the ring corresponding to the impact parameter bin, and the efficiency $\varepsilon(E_j, r_i)$ is determined by

$$\varepsilon(E_j, r_i) = \frac{N_{\text{cut}}(E_j, r_i)}{N_{\text{orig}}(E_j, r_i)}$$

where $N_{\text{orig}}(E_j, r_i)$ is the number of showers originally simulated for the primary energy (range) E_j and impact parameter (range) r_i. $N_{\text{cut}}(E_j, r_i)$ is the number of showers for the primary energy (range) E_j and impact parameter (range) r_i which survived the analysis procedure.

The curves clearly show "supercut characteristics" in that the effective area is strongly energy dependent and drops with increasing energy after steeply rising to a maximum. It is therefore impossible to determine an integral flux without prior knowledge of the shape

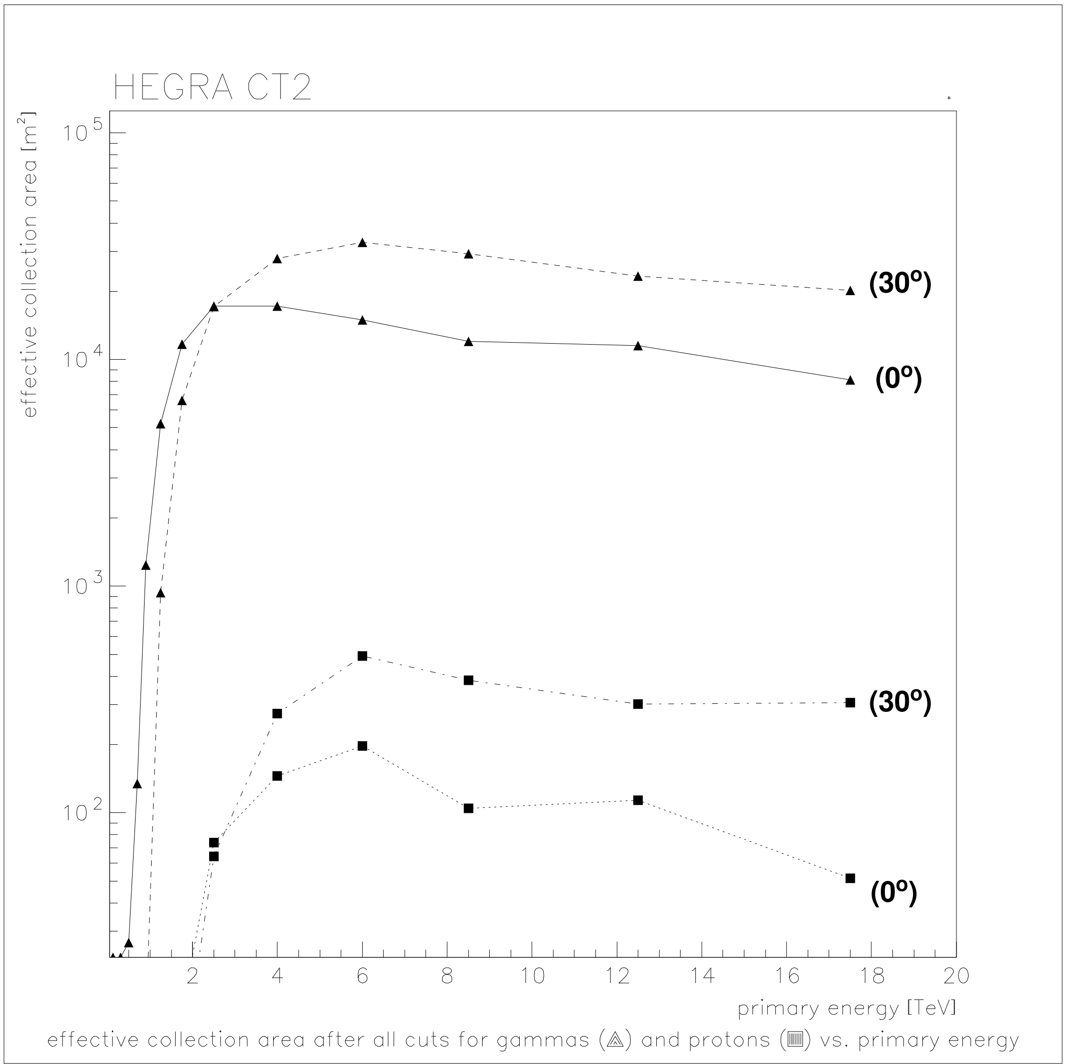

Figure 8: The effective collection area $A_{\text{eff}}(E)$ as defined in the text for gammas (triangles) and protons (squares) determined from Monte Carlo studies for CT2 for zenith angles $\theta = 0°$ and $\theta = 30°$. The photoelectron to ADC count conversion factor was taken to be $\chi_1 = 1.25$ for this plot (see text).

of the source spectrum. With a given source spectrum the flux can then be determined by convoluting the spectrum with the effective collection area function $A_{\text{eff}}(E)$ such that an expected integral rate is obtained which is then compared to the observed rate (as described in [18]).

The flux value which will be given below has two main uncertainties:

1. The absolute energy calibration of CT2 is only coarse. Here especially the Monte Carlo photoelectron to ADC count conversion factor χ_1 is uncertain. It was determined in [19] using the following method:

   The dependence of the event rate on the software trigger threshold was determined for OFF source observations from CT2. The conversion factor χ_1 was then adjusted such that the threshold-dependece of the event rate obtained in the Monte Carlo simulation of the cosmic ray rate (taking into account chemical composition) coincided with the measured dependence. This method resulted in $\chi_1 = 1.5 \pm 0.4$ ADC counts/photoelectron where the error is mainly due to the uncertainty of the measurements of the cosmic ray flux which are used in the Monte Carlo generation of the cosmic ray spectrum and uncertainties in parameters such as the effective mirror area and reflectivity, light guide transmission and the spectral variation of the quantum efficiency of the photo multipliers.

   Using a direct method discussed in [20], the photoelectron to ADC count conversion factor was however measured to be 1.0 ± 0.1 ADC counts/photoelectron. This discrepancy is not yet fully understood.

   In this analysis values of $\chi_1 = 1.25 \pm 0.25$ are considered.

2. In order to determine the flux, a spectral shape must be known. As a first approach, a continuation of the power law spectrum seen by EGRET and the Whipple group with a differential spectral index of 2.0 ± 0.2 is *assumed*.

   In order to minimize the sensitivity of the flux value to errors in the spectral index, the threshold E_{thr} for the statement of an integral flux using the method mentioned above is according to [18] best chosen as

   $$E_{\text{thr}} = E_{\text{max}} \cdot e^{-\frac{1}{\alpha-1}}$$

   where α is the "best guess" differential spectral index and E_{max} is the primary gamma energy at which the (simulated) differential detection rate has its maximum.

   E_{max} is dependent on χ_1: for $\alpha = 2.0$ and $\chi_1 = 1.25 \pm 0.25$ values of $E_{\text{max}} = 3.0 \mp 0.2$ TeV result. Therefore E_{thr} should be chosen to be 1.1 ∓ 0.1 TeV. For simplicity the threshold is chosen to be 1 TeV.

Finally, the zenith angle dependence of the effective collection area was taken into account: the average $\cos(\theta)$ for the data from CT2 with $\theta < 25°$ is 0.9592. The collection areas obtained for $\theta = 0°$ and $\theta = 30°$ were therefore combined into one effective collection area by taking the weighted average, the weights being chosen such that the correct average $\cos(\theta)$ results.

Based on the data from CT2 with $\theta < 25°$ and the rate of 6.2 h^{-1} obtained from this data, the average flux above 1 TeV from Mkn 421 in the period between 29 December 1994 and 5 May 1995 is thus calculated to be

$$1.4(\pm 0.32)_{\rm Stat}(+0.6-0.4)_{\rm Syst}\times 10^{-11}\ {\rm cm^{-2}s^{-1}}$$

under the assumption of a power law spectrum with differential spectral index of 2.0 ± 0.2. The added errors are the statistical error of the rate and the systematic errors due to the uncertainty in the energy calibration and the range of ± 0.2 of the assumed spectral index. Table 4 illustrates the dependence of the flux value on differential spectral index α and photoelectron to ADC count conversion factor χ_1.

$\alpha \setminus \chi_1$	1.0	1.25	1.5
1.8	1.59×10^{-11}	1.33×10^{-11}	1.12×10^{-11}
2.0	1.75×10^{-11}	1.36×10^{-11}	1.15×10^{-11}
2.2	1.92×10^{-11}	1.52×10^{-11}	1.19×10^{-11}

Table 4: The flux value calculated from the rate 6.2 h^{-1} for the data from CT2 at zenith angles $< 25°$ in units of $cm^{-2}s^{-1}$ and in dependence on the assumed spectral index α and the photoelectron to ADC count conversion factor χ_1.

5 Conclusion

This report describes an independent detection of Mkn 421 at energies above 1 TeV using two Cherenkov telescopes. The signals seen are 144 excess events (4.0 σ) from 37 h/37 h of ON/OFF-source observations with CT1 and 335 excess events (4.3 σ) from 60 h/60 h of ON/OFF-source observations with CT2. Taking into account the fact that some of the events are coincident, the combined excess is

$$129\ \text{(CT1 only)} + 320\ \text{(CT2 only)} + 15\ \text{(CT1+CT2 coincident)} = 464\ \text{events}$$

with an approximate significance of $(3.6^2+4.1^2+2.2^2)^{\frac{1}{2}} = 5.9$ standard deviations. (Here 3.6 is the significance obtained from CT1 after removing coincident events, 4.1 is the significance from CT2 after removing coincident events, and 2.2 is the significance obtained from the coincident events). It thus confirmes the detections published by the Whipple group and establishes Mkn 421 as a source of TeV gamma rays.

The rates derived for the whole dataset from each telescope (zenith angle range 9° - 45°) are

$$3.9 \pm 1.0\ {\rm h^{-1}}\ \text{(CT1) and } 5.6 \pm 1.3\ {\rm h^{-1}}\ \text{(CT2)}$$

while one gets

$$4.6 \pm 1.1\ {\rm h^{-1}}\ \text{(CT1) and } 7.4 \pm 1.9\ {\rm h^{-1}}\ \text{(CT2)}$$

if only the 29.5 h of observations with both telescopes running in parallel are used. These rates agree within their errors. For comparison, for the first months of 1995 the Whipple group reported an average excess rate of about 40 h^{-1} above 300 GeV [10].

The significance of the signal obtained so far is too small to say anything definite about the time dependence of the signal. However, a good agreement of both telescopes is observed and future work will try to determine a possible correlation to the nearly concurrent observations of the Whipple group.

Monte Carlo studies for CT2 have resulted in an estimation of the integral flux above 1 TeV which has large systematical errors and is of the order of 1.4×10^{-11} cm^{-2}s^{-1} (see section 4). An accurate determination of this flux is of special interest since it is in the regime above 1 TeV where it is possible to probe the IR attenuation of high energy gamma rays from distant sources such as Mkn 421 (see e.g. [7] and references therein). It is therefore planned to improve this analysis by (a) using zenith angle dependent cuts, (b) applying a pointing correction and cutting at smaller ALPHA, (c) determining the background by normalizing on the upper part of the ALPHA distribution, (d) improving the energy calibration, (e) determining the flux also from the CT1 data.

Acknowledgements

The HEGRA collaboration wishes to thank the Instituto de Astrofisica de Canarias for the permission to use the HEGRA site at the Roque de los Muchachos and its facilities. This work has been supported by the BMFT, the DFG and the CICYT.

References

[1] Fonseca, V., 1995, Proc. 24th Int. Cosmic Ray Conf., **1**, 474

[2] Lin, Y. C. et al., 1992, ApJ, **401**, L61

[3] Punch, M. et al., 1992, Nature, **358**, 477

[4] Rauterberg, G. et al., 1995, Proc. 24th Int. Cosmic Ray Conf., **3**, 460

[5] Mirzoyan, R. et al., 1994, Nucl. Instr. and Meth. **A351**, 513

[6] Krennrich, F., 1994, Towards a Major Atmospheric Cherenkov Detector III, Universal Academy Press, Tokyo, 71

[7] Biller, S.D., 1995, Astroparticle Phys., **3**, 385

[8] Kerrick, A. D. et al., 1995, ApJ, **483**, L59

[9] Macomb,, D. J., et al., 1995, ApJ, **449**, L99

[10] Lamb, R.C. et al., 1995, Proc. 24th Int. Cosmic Ray Conf., **2**, 491

[11] Cawley, M.F. et al., 1985, Exp. Astron., **1**, 173

[12] Wiedner, C.A., 1994, Towards a Major Atmospheric Cherenkov Detector III, Universal Academy Press, Tokyo, 119

[13] Cawley, M., 1993, Towards a Major Atmospheric Cherenkov Detector II, Calgary, 176

[14] Fernandez, J. et al., June 1995, internal HEGRA memo "The supercut analysis of Crab data from CT2"

[15] Reynolds, P. T. et al., 1993, ApJ, **404**, 206

[16] Li, T. P. and Ma, Y. Q., 1983, ApJ, **272**, 317

[17] Konopelko, A., Plyasheshnikov, A. Schmidt, A., Preprint N6, Lebedev Physics Institute, Moscow, 1992

[18] Aharonian et al., 1995, J. Phys. G: Nucl. Part. Phys., **21**, 419

[19] Konopelko, A. et al., MPIK-K-33-1995, submitted to Astroparticle Physics

[20] Mirzoyan et al., (in these proceedings), "A direct method to measure the photoelectron to ADC count conversion factor"